Eurographics Workshop on 3D Object Retrieval (2019)
SHREC - 3D Shape Retrieval Contest (2019)
S. Biasotti, G. Lavoué, B. Falcidieno, and I. Pratikakis (Editors)
R. C. Veltkamp (SHREC organizer)

SHREC19 Protein Shape Retrieval Contest

Florent Langenfeld[1,*], Apostolos Axenopoulos[2], Halim Benhabiles[3], Petros Daras[2], Andrea Giachetti[4] , Xusi Han[5], Karim Hammoudi[6], Daisuke Kihara[5,7], Tuan M. Lai[7], Haiguang Liu[8], Mahmoud Melkemi[6], Stelios K. Mylonas[2], Genki Terashi[5], Yufan Wang[8,9] , Feryal Windal[3], and Matthieu Montes[1,*,@]

[1]Laboratoire GBCM, EA7528, Conservatoire National des Arts-et-Métiers, 2 rue Conté, 75003 Paris, France
[2]Visual Computing Lab (VCL) team, Information Technologies Institute, Centre for Research and Technology Hellas, Greece
[3]ISEN-Lille, Yncréa, Hauts de France
[4]Department of Computer Science, Università di Verona, Strada le Grazie 15, 37134 Verona
[5]Department of Biological Sciences, Purdue University, West Lafayette, Indiana, USA
[6]Université Haute-Alsace, IRIMAS EA 7499, F-68100 Mulhouse
[7]Department of Computer Science, Purdue University, West Lafayette, Indiana, USA
[8]Complex Systems Division, Beijing Computational Science Research Center, Beijing, China 100193
[9]School of Software Engineering, University of Science and Technology China, Suzhou, Jiangsu, China 215123
[*]Track organizers
[@]Corresponding author: matthieu.montes@cnam.fr

Abstract

This track aimed at retrieving protein evolutionary classification based on their surfaces meshes only. Given that proteins are dynamic, non-rigid objects and that evolution tends to conserve patterns related to their activity and function, this track offers a challenging issue using biologically relevant molecules. We evaluated the performance of 5 different algorithms and analyzed their ability, over a dataset of 5,298 objects, to retrieve various conformations of identical proteins and various conformations of ortholog proteins (proteins from different organisms and showing the same activity). All methods were able to retrieve a member of the same class as the query in at least 94% of the cases when considering the first match, but show more divergent when more matches were considered. Last, similarity metrics trained on databases dedicated to proteins improved the results.

1 Introduction

Proteins are complex macro-molecular molecules constituted of hundreds to millions of atoms, and are usually classified according to their function in the cellular environment. They display various motions reflecting their ability to undergo conformational changes in order to achieve surficial modifications and allow specific functions. Proteins are typically represented as a set of 3D coordinates indicating the position of the atoms, considered individually as rigid spheres, and current algorithms analyses this cloud of points to extract biologically relevant data. Another useful way to represent proteins is to compute their surfaces, typically representing their surface. Detecting similarities and/or dissimilarities between protein surfaces is of main importance in drug discovery pipelines, adverse drug event prediction and in the characterization of molecular processes and diseases. However, it remains very challenging to detect and characterize such variations as the surface may fluctuate for a given protein displaying many conformations, or may be very similar among different species as proteins may have the same role.

Compared to the SHREC18 track on protein shape retrieval, this year's track is focused on the evolutionary relationships between proteins shapes. We report the results of 5 methods performances from 5 different groups 1) at the *species* level (the ability to retrieve conformations of a protein of a given species) and 2) at the *proteins* level (the ability to retrieve conformations of ortholog proteins, *i.e.* regardless of the species).

2 Dataset

The SCOPe database [FBC14; CFB17; FCB18] classifies protein domains using structural and evolutionary relationships: the 2 top levels are structure-based (Class and Fold) while the 4 bottom levels are evolutionary-based (Superfamily, Family, Protein and Species, from top to bottom). It therefore represents a useful representation of the protein domains relationships and surfaces.

We only kept SCOPe entries 1) from NMR structures whose conformers display the same number of atoms, 2) from 3 SCOPe Classes: All alpha proteins, Alpha and beta proteins (a+b) and Alpha and beta proteins (a/b), 3) with at least 4 ortholog proteins.Finally, we randomly selected domains to decrease the dataset to 5,298 domains. The solvent-excluded surfaces [Con83] were computed using EDTSurf [XZ09]. The dataset is composed of 54 and 17 classes and at the *proteins* and *species* level, respectively.

DOI: 10.2312/3dor.20191058

3 Evaluation

The evaluation were computed using a loosely adaption of the evaluation code from the SHREC15' track Scalability of Non-Rigid 3D Shape Retrieval [SBS*15].

Nearest Neighbor, First-tier and Second-tier. These parameters check the ratio of models that belong to the same class as the query. For Nearest Neighbor, the first match only is considered (excluding the identity), while the $|C|-1$ and $2*(|C|-1)$ are considered for First-tier and Second-tier parameters.

Precision-Recall plot. Precision P represents the ratio of models from class C retrieved within all objects attributed to class C, while Recall R represents the ratio of models from class C retrieved compared to $|C|$.

Mean Average Precision. Given a query, its average precision is the average of all precision values computed when each relevant object is found. Given several queries, the mean average precision is the mean of average precision of each query. It then gives in a single value the overall retrieval performance of an algorithm.

4 Participants & Methods

4.1 Combined CNN-LDS framework (ConvLDSNet) for 3D shape retrieval - Stelios Mylonas, Apostolos Axenopoulos, Petros Daras

4.1.1 Problem definition

Following the recent tendency to address many scientific tasks by exploiting the existing vast amount of data, we propose a data-driven approach for the problem of 3D protein shape retrieval. A 3D neural network (NN) has been trained on relevant datasets to learn appropriate features (descriptors) for the representation of 3D molecular shapes. The input 3D model is the SES of a protein, which has been created from the protein tertiary structure using the EDTSurf software. This software produces a high resolution watertight triangulated mesh, which is then transformed to a $32 \times 32 \times 32$ voxel model to be used as input in our method.

4.1.2 Input representation

Based on the approach of WU, SONG, KHOSLA, et al. [WSK*15], we rasterize the protein 3D model to a binary voxel grid. The 3D models of the proteins are watertight, thus the parity count method is applied for binary voxelization. A voxel v is classified by counting the number of times that a line crossing the center of the voxel intersects polygons of the 3D model surface. Ray-casting the 3D model with parallel rays, all of the voxels along the ray are classified. For an odd number of intersections, voxel v is considered interior to the model, while for an even number, outside. For a $N \times N \times N$ voxel grid resolution, where $N = 32$, we cast $N \times N = 1024$ rays, with each ray passing through N-voxel centers.

4.1.3 Proposed method

The proposed architecture is depicted in Fig. 1. This network is an extension of our last year's proposal [LAC*18], which was based on the VoxNet CNN [MS15]. The new scheme consists of two branches, where two different operations are applied to the input voxels. The first convolutional branch is identical to VoxNet CNN and consists of 2 volumetric convolutional layers, 1 max-pooling layer and 1 fully connected (FC) layer. The second branch consists of two 3D-LDS modules and a FC layer. The 3D-LDS module is a novel operation which aims to simulate the behavior of Linear Dynamical Systems (LDS) and incorporate it as a NN layer. This operation was first introduced in [DAD*18] and is extended here to the 3D domain. The features obtained by the two branches after their fully connected layers are, then, concatenated and fed to a last FC layer, which provides the output feature vector.

4.1.4 Training procedure

Two datasets have been used for training the proposed scheme; the dataset from last year's competition [LAC*18] and the MolMovDB [EMG03] dataset. Among the three runs submitted, the first one (ConvLDSNet1) resulted from training the network on SHREC18, the second one (ConvLDSNet2) from training on MolMovDB and the third one (ConvLDSNet3) from training first on MolMovDB and then fine-tuning on SHREC18. Since both datasets contain classes of proteins, we added at the end of the network a Softmax layer and trained the network on a classification task.

In all cases, a three-stage training scheme has been employed: at the first stage, the convolutional part of the network is trained, by removing the LDS-branch, while, at the second step, the LDS branch is trained by removing the convolutional one. Finally, the two branches are combined, freezing their weights and training separately the last part of the network. Subsequently, the Softmax layer is dropped and the architecture is used for feature extraction. For each previously unseen input, a feature vector is extracted. After the completion of the feature extraction, the Euclidean distance metric is used to measure the dissimilarity between two input models. Small distance values indicate that the corresponding feature vectors represent members of the same protein class.

The calculation of descriptors took on average 2.5 milliseconds per model on a GeForce GTX1070 GPU, while the average comparison time between two descriptors is 0.002 milliseconds on an Intel Core i7-6700K CPU.

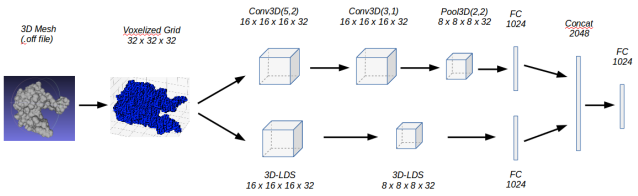

Figure 1: *The proposed architecture consisting of a convolutional branch (top) and an LDS branch (bottom).*

Acknowledgement

The work was supported by the ATXN1-MED15 PPI project funded by the GSRT - Hellenic Foundation for Research and Innovation.

4.2 Protein Shape Retrieval using 3D Zernike moments (3DZM) - Yufan Wang, Haiguang Liu

3D Zernike moments are used as the shape descriptors. The protein shapes were represented using the 3D Zernike moments by projecting each shape to the corresponding Zernike polynomials with order (n,l,m)[Can99; NK03]. To speed up the calculations, a binary file was used to store the computed Zernike moments for all 5,298 proteins. Pearson Correlation Coefficient (cc) between the query model and each protein aligned in the best orientation is used to evaluate the similarity of two shapes; the similarities are calculated between each pair, resulting in $5297 \times 5298/2$ pairs. Fast Fourier Transformation (FFT) method is used to speed up the model rotation calculation to find the best orientations that maximize the overlap of the two proteins [LHZ12; SCC*17]. The correlation coefficient cc is then computed as the similarity of the two shapes. The dissimilarity between each pair is defined as $(1-cc)$.

Data pre-processing (transforming off files into PDB files) costed nearly 1.5 hours on a computer with Intel i7 CPU 2.7GHz. Another 0.5 hour was required to convert the PDB format files to 3DZM data file. To align and compute similarities between two shapes, about 0.5 second is required; therefore, the comparison calculations lasts 4 hours using 480 Intel Xeon E5 CPUs (2.5GHz).

4.3 3D Zernike Descriptors (3DZD) - Xusi Han, Tuan M. Lai, Genki Terashi, Daisuke Kihara

Our group has submitted three runs, all of which were based on 3D Zernike Descriptors (3DZD). We represented the protein global surface information with 3D Zernike Descriptors (3DZD) and quantified the similarity between 3DZDs by either the Euclidean distance or a similarity score from neural network. 3DZD is mathematical moment-based invariants of 3D functions [SLL*08], which has been demonstrated efficient for various biomolecular structure comparisons [KSCE11]. To calculate 3DZD for each protein, the surface triangulation of solvent excluded surface was mapped onto a 3D cubic grid, where each voxel (a cube defined by the grid) was assigned either 1 or 0: 1 for a surface voxel that locates closer than 1.7 grid interval to any triangle defining the protein surface, and 0 otherwise. This 3D grid with 1s and 0s was considered as a 3D function $f(x)$, from which 3DZD was computed. On average, 3DZD calculation takes 3.48 seconds per protein.

For the first submission (3DZD1), the global surface similarity between two proteins was quantified by the Euclidean distance of their 3DZDs. A small distance value indicates that two proteins share similar global surface. In this calculation, we took the triangulated surface (.off file) for each of the 5,298 proteins as the input to 3DZD computation and generated the 121-dimensional vector for each protein. The Euclidean distances between one query protein against all other 5297 proteins were calculated and put into each row in our first distance matrix.

For the second run (3DZD2), we built a deep learning based model to quantify the similarity between protein structures. The model was trained on all proteins in the SCOPe 2.07 database. We downloaded about 274,230 protein structures from the database for training. Solvent excluded surface of each protein was generated using the EDTSurf software [XZ09]. The triangulated surface was then taken as the input to 3DZD computation, which produced 121-dimensional vector for each protein. On a high level, given a pair of protein structures, the deep learning model outputs a score between 0 and 1 indicating their similarity (the higher the score, the more similar the structures). The model consisted of an encoder whose role was to compute key features from a 3DZD vector. The encoder was a feed forward neural network consisting of three hidden layers. Each layer used ReLU as the activation function. Intuitively, each hidden layer of the encoder computes a new level of representation of the original 3DZD vector. Given two protein structures as input, the model used the encoder to compute new features for each protein's 3DZD vector. The computed features and the original 3DZD vectors of the two structures were then compared using various operations such as the Euclidean distance, the Cosine similarity, the element-wise absolute difference, and the element-wise product. The comparison results as well as additional features such as the difference in number of vertices and the difference in number of faces were together fed into a final feed forward neural network that outputs a score between 0 and 1. We used techniques such as batch normalization and dropout to improve the training process. In the training data, if two protein structures had the same protein level, they were considered as being similar. When using a Titan X GPU, the neural network took about 0.1774 seconds on average to compare two proteins (given that 3DZD vectors have been precomputed).

For the third run (3DZD3), we have used the same approach as in the second submission, except that in this case we trained the model to consider two protein structures to be similar only when the two structures have the same *species* level. In the second submission, if two protein structures have the same *proteins* level but different *species* level, we still considered them as being similar.

4.4 Histogram of Area Projection Transform (HAPT)- Andrea Giachetti

The method characterizes protein shapes with the Histograms of Area Projection Transform (HAPT) [GL12]. This descriptor, well suited for nonrigid shape retrieval and well behaving in SHREC18 contest on protein shape retrieval [LAC*18] is based on a spatial map (Multiscale Area Projection Transform) [GL12] that encodes the likelihood of the 3D points inside the shape of being centers of spherical symmetry. This map is obtained by computing, for each radius of interest, the value:

$$APT(\vec{x},S,R,\sigma) = Area(T_R^{-1}(k_\sigma(\vec{x}) \subset T_R(S,\vec{n})))$$

where S is the surface of the object, $T_R(S,\vec{n})$, is the parallel surface of S shifted along the normal vector $\vec{n}$ (only in the inner direction) and $k_\sigma(\vec{x})$ is a sphere of radius σ centered in the generic 3D point $\vec{x}$ where the map is computed. Values at different radii are normalized in order to have a scale-invariant behavior, creating the Multiscale APT (MAPT):

$$MAPT(x,y,z,R,S) = \alpha(R)APT(x,y,z,S,R,\sigma(R))$$

where $\alpha(R) = 1/4\pi R^2$ and $\sigma(R) = c \cdot R,\ \ 0 < c < 1$.

A discrete MAPT is easily computed, for selected values of R, on

a voxelized grid including the surface mesh, with the procedure described in GIACHETTI and LOVATO [GL12]. The map is computed in a grid of voxels with side s on a set of corresponding sampled radius values. For the proposed task, discrete MAPT maps were quantized in 12 bins and histograms computed at the selected scales (radii) were concatenated creating an unique descriptor. Voxel side and sampled radii were fixed set for each run and chosen to represent the approximate radii of the spherical symmetries visible in the models.

We tested three different options for the algorithm's parameters. In the first (HAPT1), we put $s = 0.5$ and we computed the MAPT histograms for 8 increasing radii starting from $R_1 = 0.5$ iteratively adding a fixed step of 0.5 for the remaining values and setting $\sigma = 0.25$. In the second (HAPT2), we put $s = 0.4$ and we computed the MAPT histograms for 10 increasing radii starting from $R_1 = 0.4$ iteratively adding a fixed step of 0.4 for the remaining values and setting $\sigma = 0.2$. In the third (HAPT3), we put $s = 0.3$ and we computed the MAPT histograms for 8 increasing radii starting from $R_1 = 0.3$ iteratively adding a fixed step of 0.3 for the remaining values and setting $\sigma = 0.15$.

The procedure for model comparison then simply consists in concatenating the MAPT histograms computed at the different scales and measuring distances between shapes by evaluating the Jeffrey divergence of the corresponding concatenated vectors. The estimation of the descriptors took 4.98 seconds on average for the first run, 11.1 seconds on average for the second run, 13.02 seconds on average for the third run on a laptop with an i7-4720HQ CPU running Ubuntu Linux 18.04. The descriptor comparison time was negligible.

4.5 A Framework towards Protein Shape Singularity Characterization (Ft-PSSC) - Halim Benhabiles, Karim Hammoudi, Feryal Windal, Mahmoud Melkemi

Our proposed retrieval method aims at exploring three different feature extraction techniques in order to reach the best performance. More specifically, the first technique is based on GASD descriptor, the second on FPFH descriptor and the last one on the combination of both descriptors. For the similarity measure, we use a L2 distance.

4.5.1 Processing pipeline

- Data pre-processing: sub-sampling and normalization of the protein point cloud. The sub-sampling reduced the number of points to approximately 20% using the simplification method BENHABILES, AUBRETON, BARKI, and TABIA [BABT13], preserving the global shape of the protein and its swiftness. The minimum bounding sphere [Wel91] of the protein was computed to rescale it into a unit sphere $S(c,r)$ where c is the center set to 0 and r is the radius set to 1. This makes each protein of the dataset invariant to geometric transformations including scale and translation.
- GASD descriptor calculation [dMT16]: the descriptor consists of firstly estimating a reference frame of the point cloud using PCA (Principal Component Analysis) approach, then exploiting the reference frame to transform the point cloud into a canonical coordinate system making it pose invariant. The final global descriptor is then fitting points of the cloud with respect to a regular grid of 3D voxels.
- FPFH global representation (VLAD-FPFH): this stage goes through significant intermediate steps since the usual FPFH descriptor is only calculated for each point of the cloud and does not directly provide a global representation of the protein.
  - Local FPFH calculation [RBB09]: calculation of an FPFH descriptor for each point of the cloud (protein). The surface normals of all the points are calculated. Each point is considered with its nearest neighbors to calculate the angular variations between the normals of all possible pairs within the neighborhood. The angular variation is based on a Darboux frame construction. This result out into a 33 dimensions' feature vector for each point of the cloud.
  - FPFH based relevant feature selection [RBB09]: select for each protein the most relevant FPFH feature vectors. Many of the calculated FPFH vectors are redundant in all the dataset and thus do not reveal prominent characteristics that allow to distinguish between protein classes. An average FPFH vector is calculated over all the dataset and a distance distribution to this average vector is calculated for each protein. The obtained distribution for each protein which is close to a Gaussian is exploited to select the outlier vectors (vectors of interest). These vectors are those out of the range $[d-\delta, d+\delta]$, where d is the mean distance within a protein and δ is set to a large value in such way to collect 0.5% of the total number of FPFH vectors.
  - Vector of Locally Aggregated Descriptors (VLAD) [JPD*12]: allows to obtain a compact global vector for each protein. We first calculate an FPFH vector-based k-means over all the dataset. Then we apply the accumulation process of local descriptors from the previous step for each protein to generate a global vector.
- Hybrid global descriptor (GASD + VLAD-FPFH): before to combine the global FPFH vector (VLAD-FPFH) with the GASD one, we apply a PCA (Principal Component Analysis) technique on each VLAD-FPFH descriptor to balance the weights of both descriptors (GASD and VLAD-FPFH) in the final hybrid descriptor (GASD-VLAD).

4.5.2 Running time

The different steps described in the processing pipeline have been coded in C/C++ using PCL [PCL] on an i7-6700HQ CPU@2.60 GHz with 32 GB of memory (running times are reported in table 1). It is worth mentioning that the written code for each step has not been optimized to run in a parallel fashion.

5 Results

5.1 Precision-Recall curves

Methods based on 3D Zernike Descriptors and the HAPT method display good precision (> 0.6, figure 2) even for high recall values (0.7). Furthermore, these methods produced very similar performances when using different descriptors comparison methods (for

Table 1: *Running times in seconds of each step of the Ft-PSSC processing pipeline obtained respectively from the smallest and biggest protein of the dataset.*

Point cloud size	Pre-processing	GASD	Local FPFH	FPFH feature selection	VLAD	Distance to all proteins of the dataset: Vector length 512	Vector length 4224	Vector length 512+512
53k	0.12	0.85	6.56	0.001	0.11	0.017	0.14	0.03
259k	1.23	4.35	128	0.009				

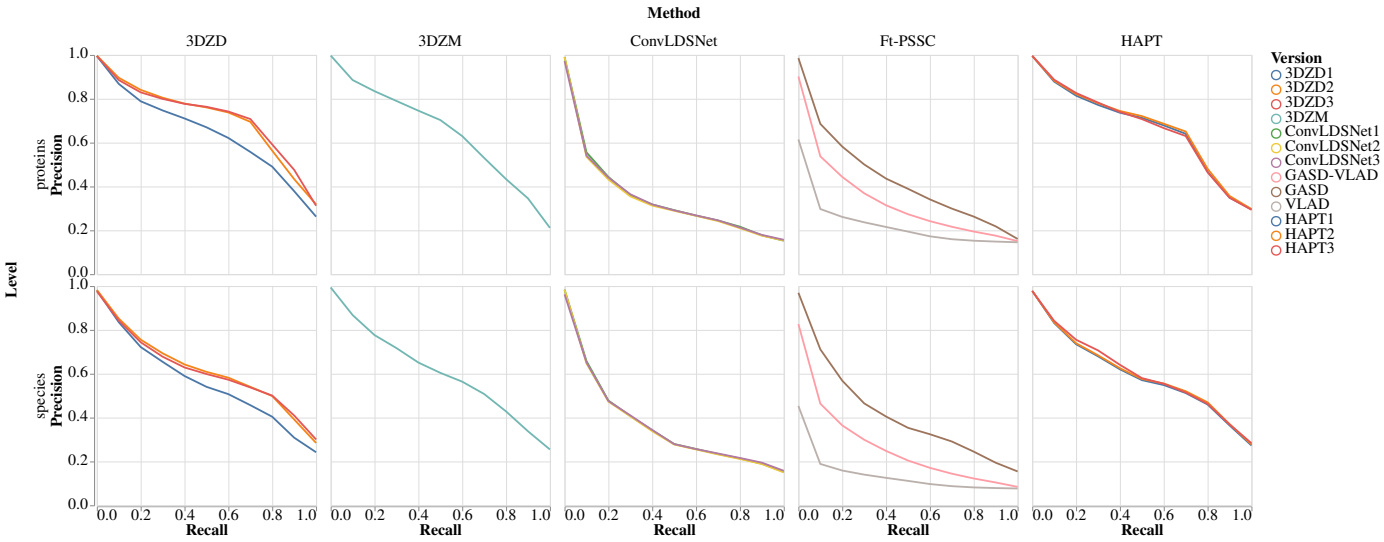

Figure 2: *Precision-Recall curves for the proteins (left) and species (right) level. For each row, the precision-recall curves of all submitted results are shown.*

3DZD) or different parameters (for HAPT). ConvLDSNet and Ft-PSSC displayed lower performances as evaluated by the precision-recall curves, with a precision decreasing more sharply as the recall increases. Using a training dataset of protein surfaces, the 3DZD approaches significantly improved the precision at medium and high recall values. Conversely, The ConvLDSNet method seems insensitive to the training set. Regarding the Ft-PSSC method, the use of the VLAD (Vector of Locally Aggregated Descriptors) technique [JPD*12] alone or in combination with the GASD method decreased the retrieval performances.

5.2 Retrieval statistics

3DZD, 3ZDM and HAPT showed really good performance at retrieving proteins at the *species* level, and were able, from a given protein shape, to retrieve a member of the same class at the *proteins* level in more than 96% of the cases. These methods also showed high first-tier (> 0.5) and second-tier (> 0.64) values. The Ft-PSSC method using the GASD descriptor displayed high Nearest-Neighbor statistics ($> 95\%$) at both *species* and *proteins* levels, but lower performances for the other statistics. The VLAD technique, when used, degraded the Ft-PSSC performances in all statistics. The training used in the 3DZD2 and 3DZD3 approaches allowed the associated results to outperform the 3DZD1 and 3DZM

Table 2: *Nearest-neighbor (NN), First Tier (1st tier), Second Tier (2d tier), Mean Average Precision (MAP) average values computed at the species level.*

Method	NN	1st tier	2d tier	MAP
3DZD1	0.961	0.528	0.641	0.556
3DZD2	0.964	0.589	0.706	0.610
3DZD3	0.951	0.577	0.716	0.605
3DZM	0.989	0.577	0.675	0.604
ConvLDSNet1	0.975	0.332	0.422	0.355
ConvLDSNet2	0.975	0.330	0.423	0.353
ConvLDSNet3	0.952	0.333	0.423	0.355
GASD-VLAD	0.688	0.266	0.385	0.245
GASD	0.955	0.382	0.467	0.405
VLAD	0.266	0.144	0.244	0.122
HAPT1	0.947	0.555	0.705	0.578
HAPT2	0.946	0.561	0.709	0.584
HAPT3	0.944	0.563	0.709	0.588

Table 3: *Nearest-neighbor (NN), First Tier (1st tier), Second Tier (2d tier), Mean Average Precision (MAP) average values computed at the proteins level.*

Method	NN	1st tier	2d tier	MAP
3DZD1	0.988	0.579	0.729	0.638
3DZD2	0.993	0.658	0.789	0.712
3DZD3	0.989	0.665	0.802	0.720
3DZM	0.994	0.583	0.706	0.649
ConvLDSNet1	0.984	0.303	0.458	0.329
ConvLDSNet2	0.984	0.296	0.457	0.324
ConvLDSNet3	0.961	0.301	0.458	0.328
GASD-VLAD	0.797	0.315	0.481	0.315
GASD	0.977	0.372	0.506	0.417
VLAD	0.390	0.226	0.380	0.206
HAPT1	0.988	0.616	0.734	0.659
HAPT2	0.988	0.624	0.738	0.666
HAPT3	0.991	0.613	0.732	0.658

approach for the first-tier, second-tier and MAP statistics at the *proteins* level, while the 3DZM approach display slightly better results for the nearest-neighbor metrics at the *species* level only. The ConvLDSNet method is little sensitive to the training set.

6 Discussion & Conclusion

In this track, we investigate the ability of the participants' methods to use biological shapes to classify proteins sharing evolutionary relationships as evaluated by the SCOPe database[FBC14; CFB17; FCB18]. The surfaces encompass only globular proteins from NMR structures, which capture conformational changes occurring at the nanosecond timescale while large conformational changes can occur at the microsecond or millisecond timescale. As a result, this dataset presents only a narrow spectrum of the protein surface diversity.

All methods except the VLAD-FPFH approach analyze global descriptors and resulted in overall good performances. These results indicate that the classification problem of a set of proteins sharing evolutionary relationships may be comprehended using a global description of protein surfaces. The only local descriptor (combining the VLAD and FPFH techniques) used in this track resulted in lesser performances. Taken together, these results suggest that proteins displaying multiple conformations (such as NMR models) share an overall common shape that is detected by global descriptors, while a local analysis identify local patterns that cannot discriminate between different proteins.

References

[BABT13] BENHABILES, H., AUBRETON, O., BARKI, H., and TABIA, H. "Fast simplification with sharp feature preserving for 3D point clouds". *2013 11th International Symposium on Programming and Systems (ISPS)*. Apr. 2013, 47–52. DOI: 10.1109/ISPS.2013.6581492 4.

[Can99] CANTERAKIS, N. "3D Zernike Moments and Zernike Affine Invariants for 3D Image Analysis and Recognition". *In 11th Scandinavian Conf. on Image Analysis*. 1999, 85–93 3.

[CFB17] CHANDONIA, JOHN-MARC, FOX, NAOMI K., and BRENNER, STEVEN E. "SCOPe: Manual Curation and Artifact Removal in the Structural Classification of Proteins – extended Database". *Journal of Molecular Biology* 429.3 (2017). Computation Resources for Molecular Biology, 348–355. ISSN: 0022-2836. DOI: https://doi.org/10.1016/j.jmb.2016.11.023. URL: http://www.sciencedirect.com/science/article/pii/S0022283616305186 1, 6.

[Con83] CONNOLLY, M. L. "Analytical molecular surface calculation". *Journal of Applied Crystallography* 16.5 (Oct. 1983), 548–558. DOI: 10.1107/S0021889883010985. URL: https://doi.org/10.1107/S0021889883010985 1.

[DAD*18] DIMOU, A., ATALOGLOU, D., DIMITROPOULOS, K., et al. "LDS-Inspired Residual Networks". *IEEE Transactions on Circuits and Systems for Video Technology* (2018), 1–1. ISSN: 1051-8215. DOI: 10.1109/TCSVT.2018.2869680 2.

[dMT16] D. M. LIMA, J. P. S. and TEICHRIEB, V. "An Efficient Global Point Cloud Descriptor for Object Recognition and Pose Estimation". *2016 29th SIBGRAPI Conference on Graphics, Patterns and Images (SIBGRAPI)*. Oct. 2016, 56–63. DOI: 10.1109/SIBGRAPI.2016.017 4.

[EMG03] ECHOLS, NAT, MILBURN, DUNCAN, and GERSTEIN, MARK. "MolMovDB: Analysis and visualization of conformational change and structural flexibility". *Nucleic acids research* 31 (Feb. 2003), 478–82. DOI: 10.1093/nar/gkg104 2.

[FBC14] FOX, NAOMI K., BRENNER, STEVEN E., and CHANDONIA, JOHN-MARC. "SCOPe: Structural Classification of Proteins—extended, integrating SCOP and ASTRAL data and classification of new structures". *Nucleic Acids Research* 42.D1 (2014), D304–D309. DOI: 10.1093/nar/gkt1240. eprint: /oup/backfile/content_public/journal/nar/42/d1/10.1093/nar/gkt1240/2/gkt1240.pdf. URL: http://dx.doi.org/10.1093/nar/gkt1240 1, 6.

[FCB18] FOX, NAOMI K, CHANDONIA, JOHN-MARC, and BRENNER, STEVEN E. "SCOPe: classification of large macromolecular structures in the structural classification of proteins—extended database". *Nucleic Acids Research* 47.D1 (Nov. 2018), D475–D481. ISSN: 0305-1048. DOI: 10.1093/nar/gky1134. eprint: http://oup.prod.sis.lan/nar/article-pdf/47/D1/D475/27437423/gky1134.pdf. URL: https://dx.doi.org/10.1093/nar/gky1134 1, 6.

[GL12] GIACHETTI, ANDREA and LOVATO, CHRISTIAN. "Radial symmetry detection and shape characterization with the multiscale area projection transform". *Computer Graphics Forum*. Vol. 31. 5. Wiley Online Library. 2012, 1669–1678 3, 4.

[JPD*12] JÉGOU, H., PERRONNIN, F., DOUZE, M., et al. "Aggregating Local Image Descriptors into Compact Codes". *IEEE Transactions on Pattern Analysis and Machine Intelligence* 34.9 (Sept. 2012), 1704–1716. ISSN: 0162-8828. DOI: 10.1109/TPAMI.2011.235 4, 5.

[KSCE11] KIHARA, DAISUKE, SAEL, LEE, CHIKHI, RAYAN, and ESQUIVEL-RODRIGUEZ, JUAN. "Molecular Surface Representation Using 3D Zernike Descriptors for Protein Shape Comparison and Docking". *Current Protein & Peptide Science* 12.6 (2011), 520–530. ISSN: 1389-2037/1875-5550. DOI: 10.2174/138920311796957612. URL: http://www.eurekaselect.com/node/88710/article 3.

[LAC*18] LANGENFELD, FLORENT, AXENOPOULOS, APOSTOLOS, CHATZITOFIS, ANARGYROS, et al. "Protein Shape Retrieval". *Eurographics Workshop on 3D Object Retrieval*. Ed. by TELEA, ALEX, THEOHARIS, THEOHARIS, and VELTKAMP, REMCO. The Eurographics Association, 2018. ISBN: 978-3-03868-053-6. DOI: 10.2312/3dor.20181053 2, 3.

[LHZ12] LIU, HAIGUANG, HEXEMER, ALEXANDER, and ZWART, PETER H. "The *Small Angle Scattering ToolBox* (*SASTBX*): an open-source software for biomolecular small-angle scattering". *Journal of Applied Crystallography* 45.3 (June 2012), 587–593. DOI: 10.1107/S0021889812015786. URL: https://doi.org/10.1107/S0021889812015786 3.

[MS15] MATURANA, D. and SCHERER, S. "VoxNet: A 3D Convolutional Neural Network for real-time object recognition". *2015 IEEE/RSJ International Conference on Intelligent Robots and Systems (IROS)*. Sept. 2015, 922–928. DOI: 10.1109/IROS.2015.7353481 2.

[NK03] NOVOTNI, MARCIN and KLEIN, REINHARD. "3D Zernike Descriptors for Content Based Shape Retrieval". *Proceedings of the Eighth ACM Symposium on Solid Modeling and Applications*. SM '03. Seattle, Washington, USA: ACM, 2003, 216–225. ISBN: 1-58113-706-0. DOI: 10.1145/781606.781639. URL: http://doi.acm.org/10.1145/781606.781639 3.

[PCL] PCL. *"Point Cloud Library"*. http://pointclouds.org. Accessed: 2019-03-08 4.

[RBB09] RUSU, R. B., BLODOW, N., and BEETZ, M. "Fast Point Feature Histograms (FPFH) for 3D registration". *2009 IEEE International Conference on Robotics and Automation*. May 2009, 3212–3217. DOI: 10.1109/ROBOT.2009.5152473 4.

[SBS*15] SIPIRAN, IVAN, BUSTOS, BENJAMIN, SCHRECK, TOBIAS, et al. "SHREC ' 15 Track : Scalability of Non-Rigid 3D Shape Retrieval". 2015 2.

[SCC*17] SONG, NA, CRACIUN, DANIELA, CHRISTOFFER, CHARLES W., et al. "Protein Shape Retrieval". *Eurographics Workshop on 3D Object Retrieval*. Ed. by PRATIKAKIS, IOANNIS, DUPONT, FLORENT, and OVSJANIKOV, MAKS. The Eurographics Association, 2017. ISBN: 978-3-03868-030-7. DOI: 10.2312/3dor.20171055 3.

[SLL*08] SAEL, LEE, LI, BIN, LA, DAVID, et al. "Fast protein tertiary structure retrieval based on global surface shape similarity". *Proteins: Structure, Function, and Bioinformatics* 72.4 (2008), 1259–1273. DOI: 10.1002/prot.22030. eprint: https://onlinelibrary.wiley.com/doi/pdf/10.1002/prot.22030. URL: https://onlinelibrary.wiley.com/doi/abs/10.1002/prot.22030 3.

[Wel91] WELZL, EMO. "Smallest enclosing disks (balls and ellipsoids)". *New Results and New Trends in Computer Science*. Ed. by MAURER, HERMANN. Berlin, Heidelberg: Springer Berlin Heidelberg, 1991, 359–370. ISBN: 978-3-540-46457-0 4.

[WSK*15] WU, Z., SONG, S., KHOSLA, A., et al. "3D ShapeNets: A deep representation for volumetric shapes". *2015 IEEE Conference on Computer Vision and Pattern Recognition (CVPR)*. June 2015, 1912–1920. DOI: 10.1109/CVPR.2015.7298801 2.

[XZ09] XU, DONG and ZHANG, YANG. "Generating Triangulated Macromolecular Surfaces by Euclidean Distance Transform". *PLOS ONE* 4.12 (Dec. 2009), 1–11. DOI: 10.1371/journal.pone.0008140. URL: https://doi.org/10.1371/journal.pone.0008140 1, 3.